Studies of Particle Motions During Slow Resonant Extraction

Chong Shik Park, James Amundson, Leo Michelotti, and Vladimir Nagaslaev

Fermi National Accelerator Laboratory, PO Box 500, Batavia, IL 60510

(Dated: August 27, 2014)

Abstract

We present here

I. INTRODUCTION

II. PHASESPACE CORRECTIONS WITH DYNAMIC BUMPS

In the previous paper [1], we discussed that a septum foil plane should be aligned with particles' entrance angles at the septum because of its finite length. This alignment of the septum foil plane should be optimized in the way to reduce particle losses due to crossing the plane from outside to inside the field region or vice versa. In the Delivery Ring, however, the septum is placed at a zero dispersion section, and all shrinking separatrices are always centered at origin during an entire extraction period. These yield that the Hardt condition, a condition to arrange separatrix geometries to superimpose them for different momenta, cannot be fullfiled. Consequently, particles' angle coordinates at the entrance of the first septum are varying in time.

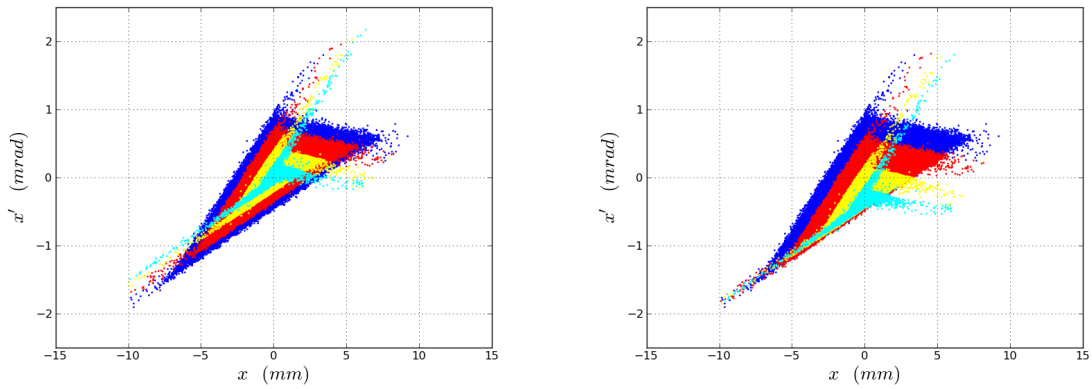

(a)Without Dynamic Bumps (b)With Dynamic Bumps

FIG. 1. Phase space plots of particles for 4 different extraction stages: (a) before and (b) after applying dynamic bump corrections

Fig. 1(a) shows a phase space of particles for 4 different extraction stages. The grey shadows are defined as the septum shadow regions in which particles will be lost [ref:M.Pullia]. Streams of unstable particles on the rightmost separatrix branch for each stage are entering the septum field region by crossing the vertical line (color:purple). As the separatrix is squeezed, these branch arms are moving upward. The septum foil plane is aligned with an initial extraction stage. Therefore, the alignment is only valid for a few turns at the begin-

ning, and there will be permanent misalignments of the septum foil plane with respect to x''s later. These result that more particles are entering the septum shadow region (color:grey shadow), and they will be lost. Variations of angle coordinates at the septum entrance will eventually be seen at the experiment target with large horizontal angular spread of extracted beams.

In order to mitigate these effects, orbit corrections are applied using 4 dynamic angle bumps. Using 4 dynamic bumps, we could align separatrices to reduce anglular deviations at the septum. Fig. 2 shows a schematic drawing of 4 dynamic bump locations in the extraction beamline. 2 bumps are located at the upstream of septa, and the other 2 are at the downstream. Upstream bumps kick particles so that outgoing particles' angles are aligned at the entrance end of the first septum during the entire extraction period. Then, downstream bumps will kick them back to original orbits.

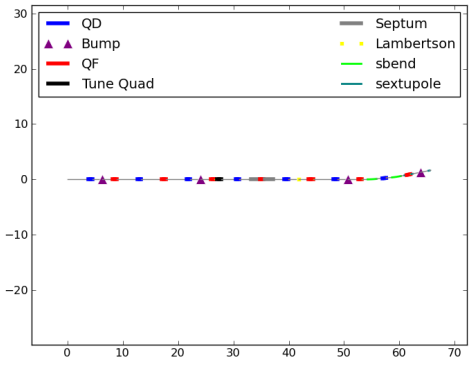

FIG. 2. Schematic drawing of the external beamline with 4 dynamic bumps.

Strengths of local orbit corrections can be easily obtained by applying the transfer matrix method with initial closed orbit conditions. Using the condition that the closed orbit is zero outside bumps, their strengths, θ_i for $i = 1, 2, 3, 4$, are given by

$$\theta_1(t) = \sqrt{\frac{\beta_s}{\beta_1}}\frac{\sin(\psi_s-\psi_2)}{\sin(\psi_2-\psi_1)}\left(-\Delta x'_s(t)\right), \quad \theta_2(t) = \sqrt{\frac{\beta_s}{\beta_2}}\frac{\sin(\psi_s-\psi_1)}{\sin(\psi_2-\psi_1)}\Delta x'_s(t),$$
$$\theta_3(t) = \sqrt{\frac{\beta_s}{\beta_3}}\frac{\sin(\psi_s-\psi_4)}{\sin(\psi_4-\psi_3)}\Delta x'_s(t), \qquad \theta_4(t) = \sqrt{\frac{\beta_s}{\beta_4}}\frac{\sin(\psi_s-\psi_3)}{\sin(\psi_4-\psi_3)}\left(-\Delta x'_s(t)\right), \tag{1}$$

where β_i's are betatron functions at the septum(s) and bumps($1, 2, 3, 4$), ψ_i's are betatron phase advances, and $\Delta x'_s(t)$ is required changes of angle coordinates at the septum entrance as a function of time. Fig. 3 shows changes of bump strengths in time. Since particles' entrance angles to the septum are aligned to the initial extraction stage, bump strengths are zero at the beginning and are maximum at the end of extraction.

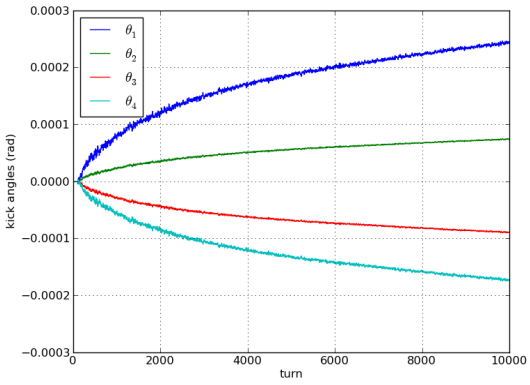

FIG. 3. Strength changes of dynamic bumps in time.

Before applying dynamic bumps, phase space of circulating particles are centered at the origin as shown in Fig. 1. As the separatrix is squeezed by increaing tune-quad strengths, phase space areas are shrinking in time and outgoing branches.

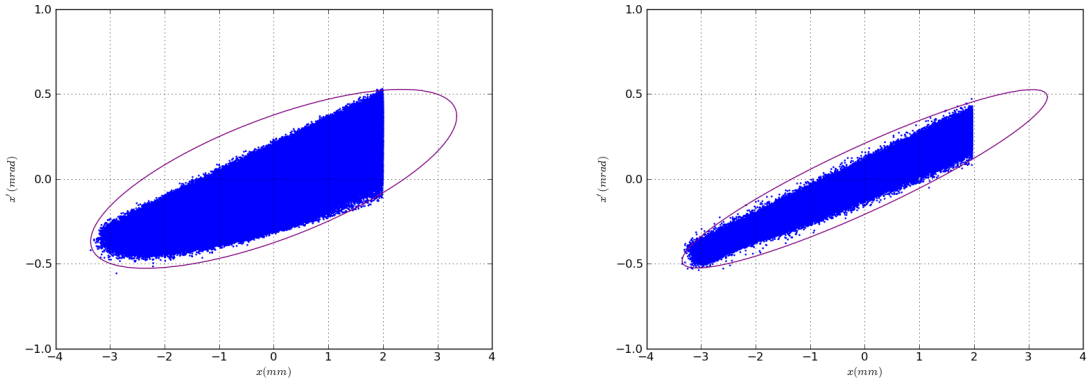

(a)Without Dynamic Bumps (b)With Dynamic Bumps

FIG. 4. Footprints of extracted particles with/without dynamic bumps.

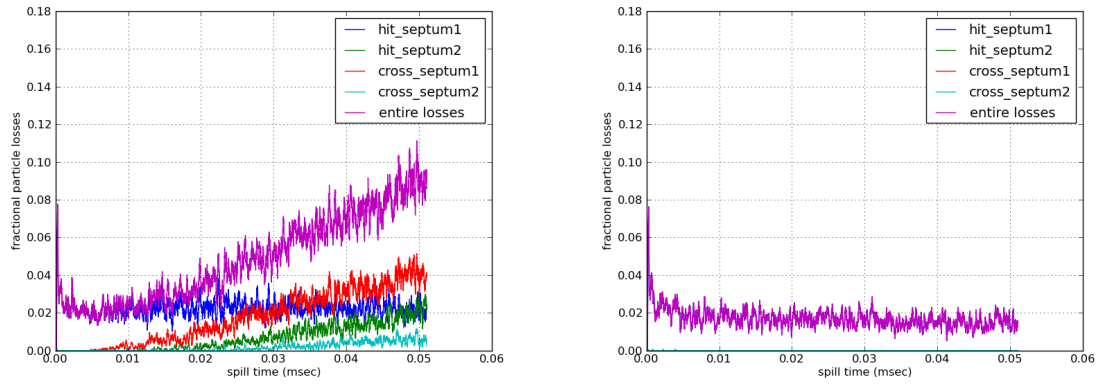

(a)Without Dynamic Bumps (b)With Dynamic Bumps

FIG. 5. Particle losses in time with/without dynamic bumps.

III. TRACKING OF PARTICLE LOSSES

IV. EMITTANCE GROWTH RATES WITH RFKO BEAM HEATING

V. RFKO BEAM DISTRIBUTION FUNCTION

VI. ARRIVAL TIME DISTRIBUTION

VII. CONCLUSION

VIII. ACKNOWLEDGMENTS

---

[1] C.S. Park, "Tracking Simulation of the Third-Integer Resonant Extraction for the Fermilab Mu2e Experiment," submitted to PRST-AB.